Elementary Steps of Enzymatic Oxidation of Nifedipine Catalyzed by Horseradish Peroxidase

Maria S. Afanasyeva,*,† Marc B. Taraban,† Nikolay E. Polyakov,† Peter A. Purtov,† Tatyana V. Leshina,† and Charles B. Grissom‡

Institute of Chemical Kinetics and Combustion, Novosibirsk-90, 630090 Russia, and Department of Chemistry, University of Utah, 315 South 1400 East, Salt Lake City, Utah 84112-0850

Received: July 27, 2006; In Final Form: August 28, 2006

The elementary steps of the enzymatic oxidation of nifedipine (NF) catalyzed by horseradish peroxidase (HRP) have been described based on analysis of kinetic magnetic field effects (MFEs). It has been shown that the first step of the catalytic cycle is single electron transfer resulting in formation of $NF\bullet^+$ radical cation and ferroperoxidase (Per^{2+}). As a result, comparison with an earlier studied oxidation reaction of NADH catalyzed by HRP evidenced that the enzymatic oxidations of two substrates—native, NADH, and its synthetic analogue, NF—catalyzed by HRP in the absence of H_2O_2 follow identical mechanisms.

Introduction

Involvement of paramagnetic intermediates in the catalytic cycle of oxidation of organic substrates by many metalloenzymes has already become a widely accepted viewpoint. The most spectacular examples in this regard are heme-containing enzymes where multispin states of the central iron atom in the active site stipulate strict sequence of transformations of active enzyme intermediates.[1,2]

Participation of paramagnetic intermediates of HRP, such as Comp I, Comp II, Comp III, and ferroperoxidase (Per^{2+}), in the enzyme catalytic cycle are favorable preconditions for application of spin chemistry techniques,[3] in particular, magnetic field effects (MFEs), to study the elementary mechanisms of HRP-catalyzed oxidations of different substrates.

Of special interest are attempts to use spin chemistry techniques to elucidate the role of paramagnetic intermediates in the enzymatic processes involving one of the most intriguing biological substrates, NADH, which is still debated in the literature.[4] Two possible mechanisms of NADH oxidation in enzymatic or nonenzymatic reactions are one-step hydride transfer and a multistage process initiated by a single electron-transfer step followed by formation of radical ion pairs as transient species. Reference data show a lot of evidence in support of one-step hydride transfer oxidation.[5] However, it has been demonstrated also that strong one-electron oxidants could initiate formation of radical ion pairs involving the radical cation of NADH.[6] This process is also more favored in reactions with such powerful oxidants as iron-containing enzymes, e.g., catalase.[7] Indeed, recent studies have illustrated applications of spin chemistry techniques to demonstrate the involvement of radical stages in the NADH oxidations catalyzed by HRP.[8,9] In addition, an overwhelming amount of useful information on detailed mechanisms of the aromatization of the 1,4-dihydropyridine moiety of NADH to the pyridine one in NAD^+ has been obtained from investigations of chemically induced dynamic nuclear polarization (CIDNP) in oxidation reactions of synthetic analogues of NADH, substituted 1,4-dihydropyridines (1,4-DHPs), by organic electron acceptors.[10−13] The present paper is devoted to the first attempt to employ the magnetic field effects to study the enzymatic oxidation of the synthetic NADH analogue, 1,4-dihydro-2,3-dimethyl-3,5-dicarbmethoxy-4-nitrophenyl pyridine (nifedipine, NF), catalyzed by HRP.

The main goal of the present paper is to elucidate the involvement of the single-electron-transfer step between NF and the oxidant (native HRP), which is believed to initiate the nonenzymatic oxidation of 1,4-DHPs[10−13] and has been earlier detected in the enzymatic oxidation of NADH.[9] Note that NF was chosen as the substrate to react with HRP since it is one of the vast family of various 1,4-DHPs reacting with HRP within a convenient range of effective reaction rates. It is necessary to note that heretofore the single electron reduction of HRP by NADH as the first stage of the catalytic cycle is quite uncommon since it was believed that the reduced form of HRP, Per^{2+}, was generated only in a side reaction of the HRP catalytic cycle.[14] However, the existence of the reduction step of HRP to its ferroperoxidase intermediate in the reaction of photoexcited NADH and HRP was earlier demonstrated by Zhabotinsky.[15]

Experimental Section

Reagents. HRP (type XII, 250−330 U/mg, R/Z > 3.1) was purchased from Sigma, Inc. and used without further purification. NF was from Sigma. Potassium hydrogen phosphate (K_2HPO_4), potassium dihydrogen phosphate (KH_2PO_4), ethanol (C_2H_5OH) (EtOH), as well as deuterated solvents (methyl alcohol (CD_3OH) (99%) and water (D_2O) (99.9%)) were obtained from Aldrich. The antraquinone-2,6-disulfonic acid disodium salt (Q) was purchased from Reachim.

Stopped-Flow Kinetic Experiments. For stopped-flow kinetic experiments the solution of HRP was prepared in 100 mM potassium buffer made by titration of a KH_2PO_4 solution to pH = 7.0 with K_2HPO_4. The concentration of HRP was determined spectrophotometrically using a molar extinction coefficient of 102 mM^{-1} cm^{-1} at 403 nm and was 1.0 μM after mixing. The saturated NF solution was made by addition of excess NF to

* To whom correspondence should be addressed. Phone: (383)3331405. Fax: (383)3307350. E-mail: afanasieva@ns.kinetics.nsc.ru.
† Institute of Chemical Kinetics and Combustion.
‡ University of Utah.

10.1021/jp064785s CCC: $33.50
Published on Web 09/29/2006

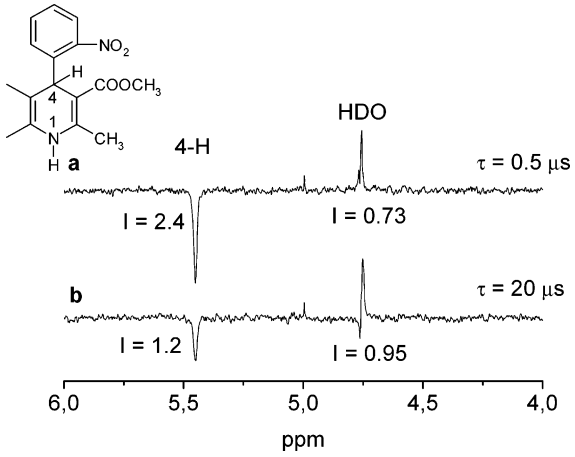

Figure 1. Nuclear polarization effects detected in the photolysis of the NF (3 mM) in the presence of Q excess (10 mM) in CD_3OH + D_2O (2:1). (a) CIDNP spectrum of the solution under study ($\tau = 0$ μs delay, 256 scans, 1 μs rf pulse duration). Line assignments: 4-H NF, 5.45 ppm, emission, $I = 2.4$; HDO, 4.75 ppm, absorption, $I = 0.73$. (b) CIDNP spectrum of the solution under study ($\tau = 20$ μs delay, 256 scans, 1 μs rf pulse duration). Line assignments: 4-H NF, 5.45 ppm, emission, $I = 1.2$; HDO, 4.75 ppm, absorption, $I = 0.95$.

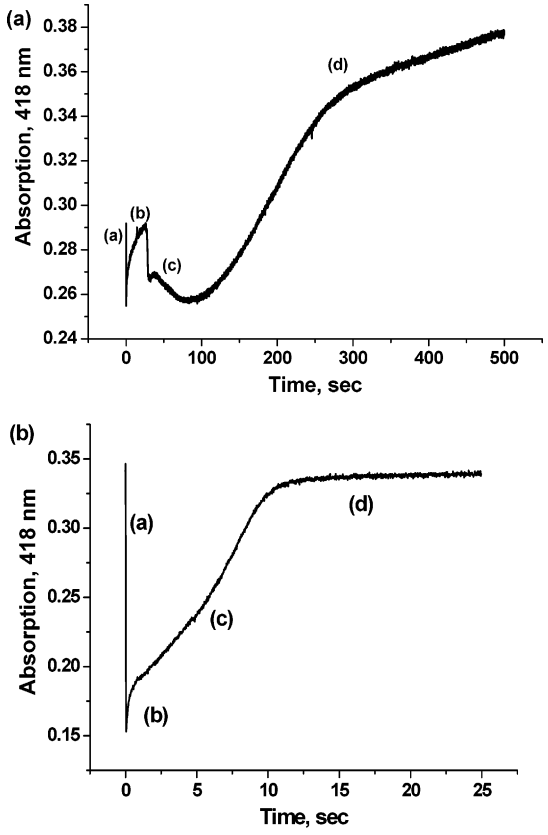

Figure 2. (a) Kinetic trace of chemical transformations observed in NF oxidation catalyzed by HRP digitally extracted at 418 nm. Reaction conditions (all concentrations after mixing): 100 mM potassium buffer, pH = 7.0; [HRP] = 1.0 μM; [NF] = 15.0 μM; 15% EtOH (v/v); 25.0 °C. (b) Kinetic trace of chemical transformations observed in NADH oxidation catalyzed by HRP extracted at 418 nm. Reaction conditions (all concentrations after mixing): MES buffer, pH = 5.56; [HRP] = 1.0 μM; [NADH] = 100 μM; 25.0 °C.

the mixture of the phosphate buffer and EtOH (5:1 v/v). The resulting solution of solubilized NF was filtered, and its final concentration was determined spectrophotometrically using a molar extinction coefficient of 6300 M^{-1} cm^{-1} at 340 nm and

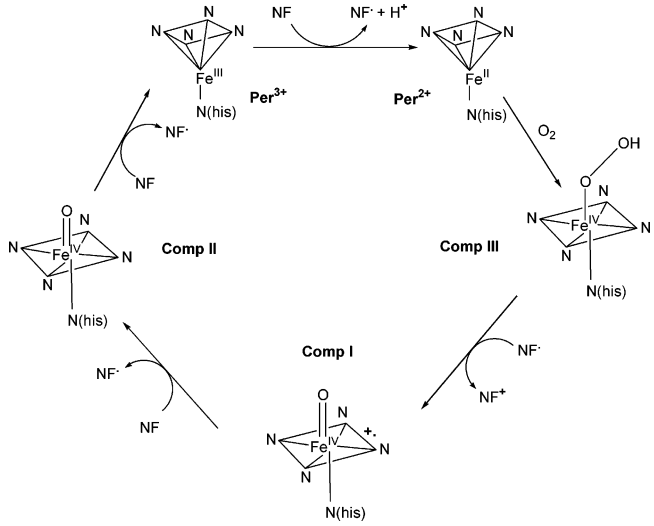

Figure 3. Catalytic cycle of NF oxidation catalyzed by HRP.

was equal to 15.0 μM after mixing. All solutions except phosphate buffer were prepared fresh daily.

Pre-steady-state kinetic experiments were carried out with a rapid-scanning stopped-flow spectrophotometer (OLIS-RSM) that can record a full absorbance spectrum at 1 kHz. The instrument has a mixing dead time of 1.3 ms as determined with dichloroindophenol and ascorbate. A circulating water bath maintains the temperature of the drive syringes and reaction cuvette (1.7 cm optical path) at 25 °C. The OLIS-RSM stopped-flow spectrophotometer was modified to position the reaction cuvette in the air gap of an electromagnet that produces an adjustable magnetic field in the range of 0−4500 G.[16] Absorbance spectra were recorded from 310 to 600 nm at a sampling rate of 1 kHz. Prior to mixing, equal amounts of enzyme and substrate solutions were kept in separate syringes. The outputs from the spectrophotometer consisted of the biphasic kinetic traces that were collected over at least 500 s at a sampling rate of 1 scan/s for NF oxidation reactions. Kinetic traces were extracted by digitally selecting the change in absorbance at 418 nm. The magnetic field strength was varied from 10 to 1000 G. Before recording data for each stopped-flow shot at a nonzero magnetic field value, a stopped-flow shot at 0 G was recorded as a control. Zero Gauss is defined as 0 G applied laboratory magnetic field and contains a geomagnetic field component that is approximately 0.3 G in Utah. Kinetic data from the spectrophotometer were stored on disk for later analysis.

Photo-CIDNP Experiments. The solution for the time-resolved photo-CIDNP experiment was prepared by addition of precise shots of NF and Q to the solvent containing CD_3OH and D_2O in volume proportion 2:1. The final concentrations of NF and Q were equal to 3 and 10 mM, respectively. In CIDNP experiments, a sample of a solution of NF and Q in a standard 5 mm Pyrex NMR tube was irradiated directly in the probe of the NMR spectrometer at room temperature. A Lambda Physik EMG 101 MSC excimer laser operating at $\lambda = 308$ nm with an average pulse energy of 100 mJ was used as a light source. In the photochemical reaction, CIDNP spectra were acquired using a DPX 200 Bruker NMR spectrometer operating at 200 MHz ^1H frequency. In time-resolved CIDNP experiments, we employed a standard nuclear spin presaturation technique to suppress the equilibrium signals. The time-resolved CIDNP experiments were carried out with a 1 μs rf detection pulse and 0 and 20 μs time delays between each laser flash and registration. The photo-CIDNP spectrum of NF in the presence of Q is shown in Figure 1a and b. CIDNP spectra include two

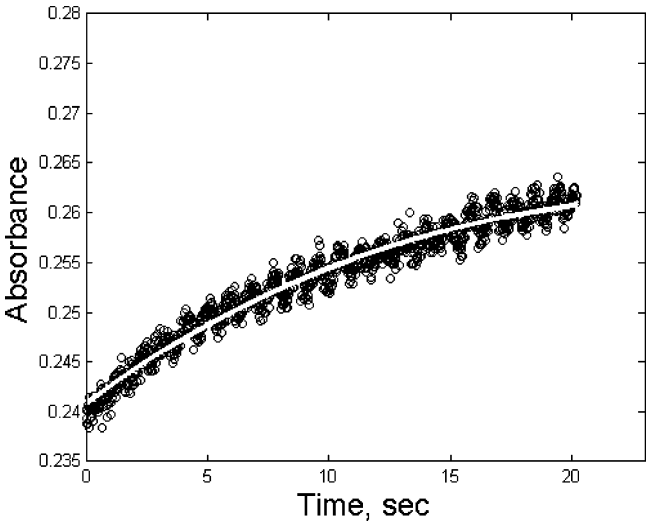

Figure 4. MatLab 6.5 for Windows fitting of the experimental data using model function eq 8. The extracted values of k_1 and k_2 (in s^{-1}) are the effective reaction rate constants: (○) experiment and (—) model fitting function.

lines: (a) emission signal at 5.45 ppm from 4-H of NF (relative intensity, *I*, is 2.4) and absorption signal at 4.75 ppm from the HDO (relative intensity, *I*, is 0.73) and (b) emission signal at 5.45 ppm from 4-H of NF (relative intensity, *I*, is 1.2) and absorption signal at 4.75 ppm from the HDO (relative intensity, *I*, is 0.95).

Results and Discussion

Stopped-Flow Kinetic Traces. When considering the formation and decay of the active intermediates of HRP we followed the earlier employed procedure for analysis of characteristic stopped-flow kinetic traces at 418 nm.[9] The stopped-flow kinetic trace for HRP-mediated NF oxidation reaction is presented in Figure 2. Taking into account the molar extinctions of HRP and its reactive intermediates measured for isolated species,[17] the interconversion of HRP's intermediates might be explained as follows (Figure 3).

It is suggested that the lowest absorption point of the initial portion of the kinetic trace (a, Figure 2a) is associated with the single-electron-transfer step, i.e., the electron is transferred from the NF (electron donor) to the native HRP (electron acceptor), resulting in ferroperoxidase (Per^{2+}) ($\epsilon_{418} = 62\ mM^{-1}\ cm^{-1}$) and $NF\bullet^+$ radical cation. As it already mentioned above, formation of radical ion pair (Per^{2+} $NADH\bullet^+$) through photoinduced electron-transfer reaction between native HRP and NADH has been demonstrated already by Zhabotinsky.[15] In the present study, the suggestion of the electron transfer being the initial step of the enzymatic oxidation is verified by analysis of magnetic field effects discussed below.

Further distinct increase of the absorption (b, Figure 2a) occurs due to reaction of ferroperoxidase with the dissolved oxygen, resulting in Comp III ($\epsilon_{418} = 115\ mM^{-1}\ cm^{-1}$). Deprotonation of $NF\bullet^+$ cation radical gives rise to formation of NF• radical, which when reacting with Comp III leads to a dramatic drop in absorption (c, Figure 2a) that is stipulated by formation of Comp I ($\epsilon_{418} = 35\ mM^{-1}\ cm^{-1}$). One-electron reduction of Comp I by the second molecule of NF brings about Comp II appearance ($\epsilon_{418} = 115\ mM^{-1}\ cm^{-1}$) and as a result a very fast absorption growth (d, Figure 2a). Fast regeneration of the native enzyme (through reaction of Comp II and NF) is not observed probably due to lowering the enzyme activity because of different radicals attack.[14]

Thus, the analysis has shown that the observed kinetic trace could be described by the same reaction sequence which has been earlier proposed for the enzymatic oxidation of NADH catalyzed by HRP,[9] although it is worth emphasizing that each elementary step in NF oxidation by HRP is more prolonged than in the case of NADH oxidation by the same enzyme (cf. Figure 2b). This fact could be reliably explained by a number of factors, such as lower concentration of NF as compared to the experiments with NADH (15 vs 100 μM), use of phosphate buffer at pH = 7.0 vs MES buffer at pH = 5.56, wherein HRP is well known to be more active, as well as addition of EtOH for solubilization of NF which is capable of producing additional slight inhibition of the enzyme. All the above-mentioned factors undoubtedly influence the enzyme activity and kinetic trace pattern.

Fitting Model. The approach for fitting the kinetic trace of the NF oxidation reaction by HRP (Figure 2a) is as follows. Since reactions of ferroperoxidase (a, Figure 2a) and Comp I (c, Figure 2a) formation are too fast for quantitative treatment under the experimental conditions, these steps are excluded from the fitting model. Therefore, in accordance with the above-described sequence of interconversions of active HRP's intermediates, part of the kinetic curve (b, Figure 2a) can be fitted to the kinetic model of two sequential first-order pseudo-unimolecular reactions

$$Per^{2+} \xrightarrow{k_1} CompIII \xrightarrow{k_2} CompI \tag{1}$$

The sequence of the reactions is described by the following system of ordinary differential equations

$$\frac{d[Per^{2+}]}{dt} = -k_1[Per^{2+}] \tag{2}$$

$$\frac{d[CompIII]}{dt} = k_1[Per^{2+}] - k_2[CompIII] \tag{3}$$

$$\frac{d[CompI]}{dt} = k_2[CompIII] \tag{4}$$

To fit the part of the kinetic trace (b, Figure 2a) it is necessary to obtain the analytical expressions describing the concentrations of the HRP intermediates in the course of their interconversions under NF oxidation

$$[Per^{2+}] = [Per^{2+}]_0 \exp(-k_1 t) \tag{5}$$

$$[CompIII] = \frac{[Per^{2+}]_0 k_1(\exp(-k_1 t) - \exp(-k_2 t))}{k_2 - k_1} \tag{6}$$

$$[CompI] = [Per^{2+}]_0 - [Per^{2+}] - [CompIII] \tag{7}$$

Since at 418 nm the molar extinction of Comp I is ca. 3 times lower and that of Per^{2+} is ca. 2 times lower than that for Comp III, the final function for fitting the experimental absorption change can be written as follows

$$A(418) = [CompIII] + \frac{[Per^{2+}]}{2} + \frac{[CompI]}{3} = \frac{[Per^{2+}]_0}{3} + \frac{[Per^{2+}]}{6} + \frac{2[CompIII]}{3} \tag{8}$$

The Levenburg−Marquardt nonlinear least-squares fitting algorithm of Matlab 6.5 for Windows was used to fit the

SCHEME 1: Spin Evolution and Processes in the Bulk for Radical Particles NF•$^+$ and Q•$^-$

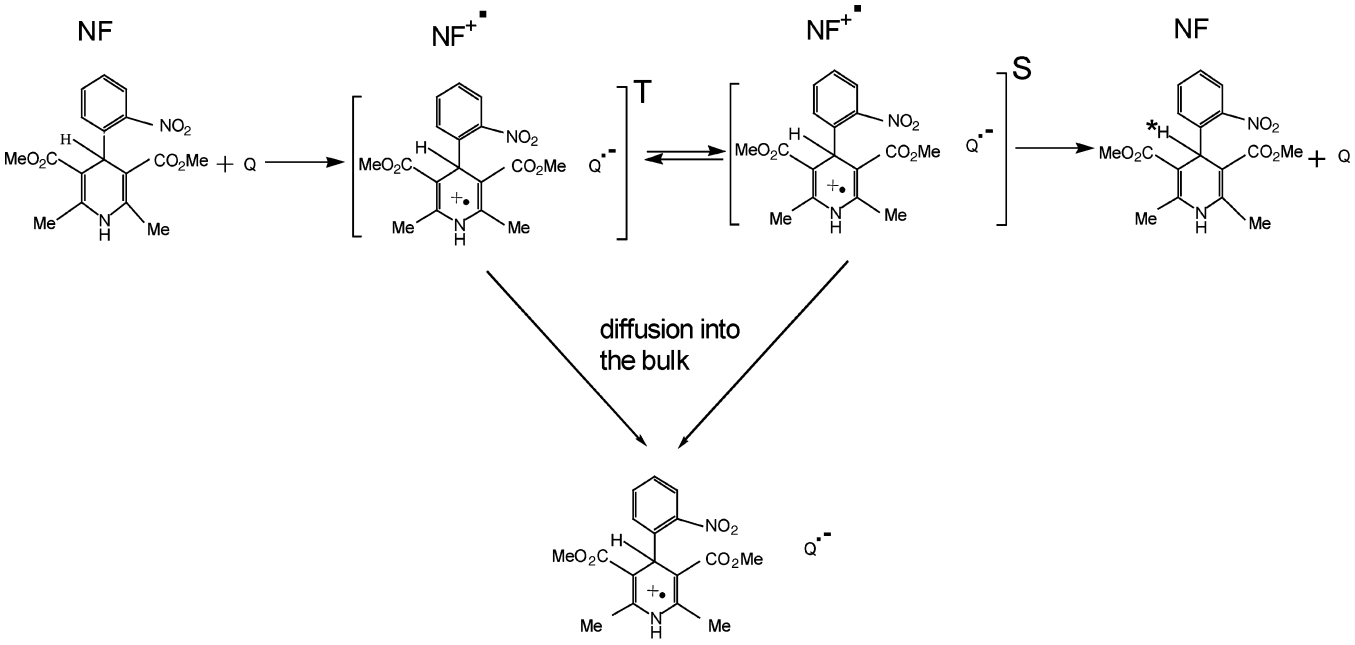

Process in the bulk

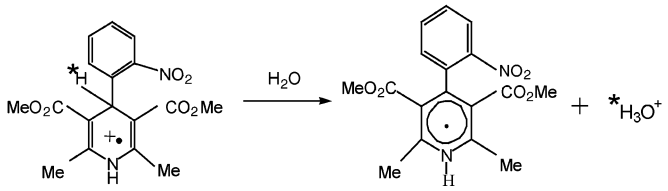

experimental data and extract values of k_1 and k_2. Figure 4 shows good agreement between the experimental kinetic trace and fitted function (eq 8).

Thus, the above results describing the kinetics of NF oxidation catalyzed by HRP allowed us to suggest the following sequence for HRP intermediates transformation

$$\text{Per}^{2+} \xrightarrow{O_2} \text{CompIII} \xrightarrow{\text{NF}\bullet} \text{CompI}$$

Here, Per^{2+} is formed through the single-electron-transfer stage between HRP and NF to form the pair of paramagnetic intermediates (Per^{2+} NF•$^+$). To confirm the existence of the initial single-electron-transfer step in the HRP-mediated process of the NF oxidation reaction, we applied spin chemistry methods.

Photoinduced Electron-Transfer Reaction between NF and Q. Analysis of magnetic field effects (MFEs) takes into account data on the electron spin density distribution in NF•$^+$ radical cation and the time scale of its lifetime. This information has been obtained from time-resolved CIDNP data observed in the model reaction of photoinduced electron transfer between electron donor, NF, and electron acceptor, antraquinone-2,6-disulfonic acid disodium salt (Q).

In the time-resolved photo-CIDNP experiment, reaction of NF oxidation by Q has shown polarization effects pointing to the presence of radical stages. Photo-CIDNP spectra of NF with Q are shown in Figure 1a and b. CIDNP spectra include two lines: the emission signal in the region of 4-H of NF at 5.45 ppm and absorption signal of HDO at 4.75 ppm. It is worth noting that polarization of the 4-H signal of NF decreases (I = 2.4 vs 1.2) with the increase of time delay (0 vs 20 μs), thus, leading to the conclusion that the observed CIDNP result from back electron transfer in a primary radical ion pair (NF•$^+$ Q•$^-$), while the appearance of the absorption signals of HDO at 4.75 ppm points to formation of a neutral radical of NF (NF•) (Scheme 1).

The outcome of this experiment is the conclusion that the appearance of CIDNP effects of 4-H of NF is evidence of the maximum value of the hyperfine interaction constant of this proton in NF•$^+$ radical cation. This, in turn, points to the similarity of the spin density distribution in NF•$^+$ and NADH•$^+$ radical cations.[18] Moreover, CIDNP observation in the radical pair involving NF•$^+$ indicates that the lifetime of the radical cation lies within the nanosecond time scale[3] and, thus, is adequate for formation of magnetic field effects in processes where NF plays the role of an electron donor.

Magnetic Field Effects. To investigate the influence of the external magnetic field on interconversion of active paramagnetic intermediates of HRP catalytic cycle stopped-flow kinetic traces of NF oxidation catalyzed by HRP were collected in a random order of magnetic field strengths in the range from 0 to 1000 G. Each kinetic trace was processed using the fitting function (eq 8) integrated in the algorithm of Matlab 6.5 for Windows. As a result, the values of effective rates k_1 and k_2 were extracted, and similar to reaction of NADH oxidation by HRP,[9] it has been found that only the first effective rate k_1 (eq 1) demonstrates a noticeable dependence on the external magnetic field strength, which is presented in Table 1 and shown in Figure 5.

As for the dependence of both effective rates on the external magnetic field strength and the nature of these dependences, a

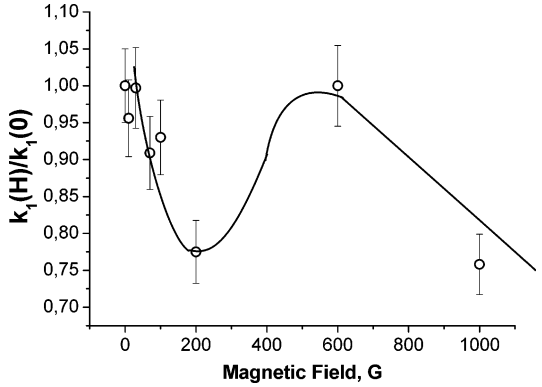

Figure 5. Magnetic field effect on the rate constant k_1 of the NF oxidation catalyzed by HRP. Error bars show the sum of 3.5% deviation of the instrumental mean error and standard deviation after average of three experimental series each with 5−6 measurements at each magnetic field strength. Reaction conditions (all concentrations after mixing): 100 mM phosphate buffer, pH = 7.0; [HRP] = 1.0 μM; [NF] = 15.0 μM; 15% EtOH (v/v); 25.0 °C.

TABLE 1: Magnetic Field Effect on the Rate Constants k_1 and k_2 of the NF Oxidation Catalyzed by HRP

H, G	k_1(H)/k_1(0)	k_2(H)/k_2(0)
0	1 ± 0.05	1 ± 0.05
10	0.956 ± 0.052	1.043 ± 0.0565
30	0.997 ± 0.0548	1.028 ± 0.0562
70	0.909 ± 0.0495	1.023 ± 0.0553
100	0.93 ± 0.0507	1.009 ± 0.0546
200	0.775 ± 0.0426	1.052 ± 0.057
600	1.0 ± 0.0547	0.983 ± 0.0531
1000	0.758 ± 0.041	0.922 ± 0.0496

possible reason for the observed distinction between k_1 and k_2 could be understood when comparing the experimentally detected field dependence with the calculated one.

To define the elementary stages of the complex chemical and/or biochemical processes one usually compares the experimental dependences of the rates of the processes under study or the yields of reaction products on the external magnetic field strengths with the dependences which are theoretically calculated under certain assumptions.[3] In the present case, the experimental dependence shown in Figure 5 is in good agreement with the modeled dependence calculated for the pair of nifedipine radical

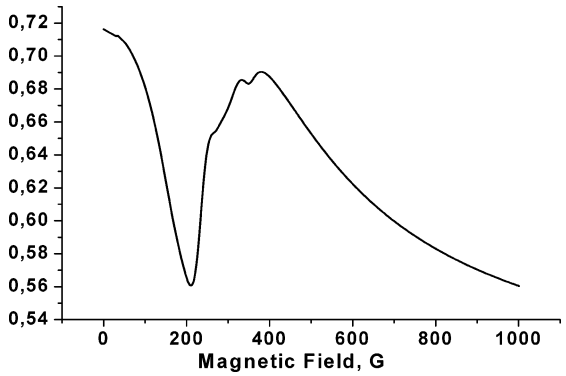

Figure 6. Dependence of the calculated escape probability for the paramagnetic pair (Per^{2+} $NF\bullet^{+}$) on the external magnetic field strength which reflects the generation of Per^{2+}, the precusor of Comp III in the catalytic cycle, and, thus, modeling the observed MFEs on the effective rate k_1.

cation $NF\bullet^{+}$ and ferroperoxidase Per^{2+} which reflects the probability of Per^{2+} to escape recombination followed by its transformation to Comp III (Figure 6). The coincidence of the model calculations with experiment shows that the magnetic field effect on k_1 for both NADH[9] and NF is generated as a result of transitions between quartet and doublet spin states in the paramagnetic pair of $NADH\bullet^{+}$ or $NF\bullet^{+}$ and Per^{2+}. Back electron transfer in the above pair occurs from the doublet spin state and leads to recovery of the native HRP, whereas the quartet spin state is the source of Compound III which is formed in accordance with the proposed scheme through reaction of ferroperoxidase and dissolved oxygen (Figure 7). Thus, the effective rate k_1 shows the dependence on the external magnetic field to the extent that it influences the effective rate for formation of ferroperoxidase Per^{2+} as a result of the electron transfer between native HRP and nifedipine NF. The absence of the MFEs at the consequent stages is most likely stipulated by the fact that the rate of reaction of Per^{2+} and O_2 is known to be within the kinetic limit rather than the diffusion one (6×10^4 M^{-1} s^{-1}).[14] It is known that the appearance of magnetic field effects formed in accordance with radical pair theory is possible for processes within the diffusion limit.[3] An adaptation of the radical pair theory used to calculate the MFEs in the multispin systems including the reaction under study is detailed earlier.[9]

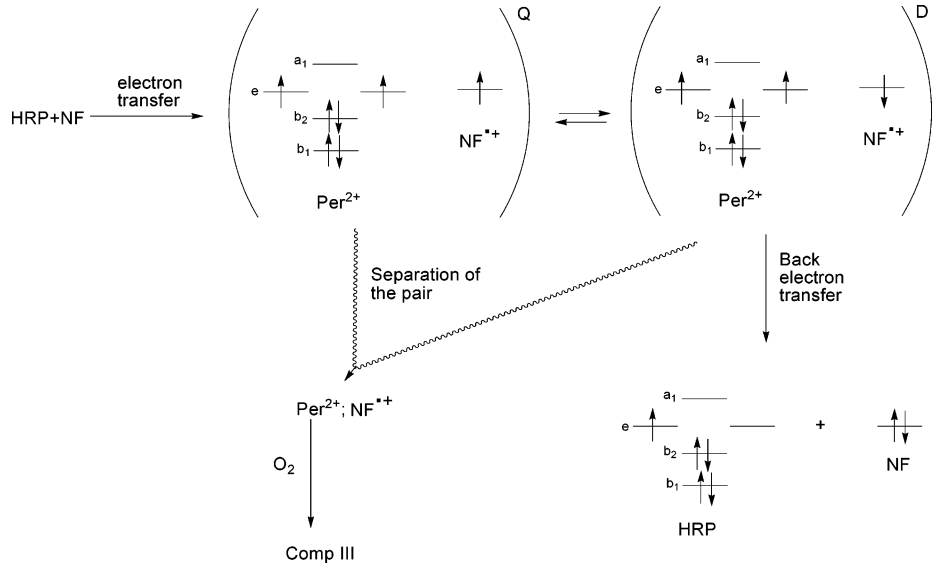

Figure 7. Spin evolution in the pair of Per^{2+} and $NF\bullet^{+}$. Q and D are quartet and doublet spin states of the paramagnetic pair $(Per^{2+}\ NF\bullet^{+})^{Q,D}$. Electronic structures of the ferroperoxidase Per^{2+} and HRP are drawn on the basis of the splitting in the distorted tetrahedral crystal field.

Conclusions

Analysis of the kinetics of NF oxidation catalyzed by HRP as well as the influence of the external magnetic field on this process allows us to suggest the sequence for the transformations of active HRP's intermediates presented in Figure 3. Note that the proposed single electron reduction of HRP to ferroperoxidase (Per^{2+}) by different donor substrates as the first stage of the catalytic cycle is quite uncommon since it was considered that Per^{2+} is generated only in the side reaction of the HRP catalytic cycle.[14] Reaction of ferroperoxidase formation through a single electron transfer between NF and native heme-containing HRP is the second example for involvement of an initial electron-transfer reaction into the HRP catalytic cycle. The suggested single-electron-transfer step was earlier demonstrated in the NADH oxidation reaction by HRP to form Per^{2+} and $NADH^{\bullet+}$ cation radical.[9] Moreover, of special interest is also confirmation of a multistage mechanism of the enzymatic oxidation of NADH and its synthetic analogue, nifedipine, so-called the electron−proton−electron or ECE (electron−chemical−electron) mechanism. Thus, in conclusion, it could be emphasized that both enzymatic oxidations of natural HRP's substrate, NADH, and its synthetic analogue, nifedipine, by HRP proceed via formation of similar paramagnetic pairs, i.e., the mechanisms of NADH and NF oxidations catalyzed by HRP are identical.

Acknowledgment. This work has been supported by grants from the U.S. Civil Research and Development Foundation (RC2-2390-NO-02) and the Russian Foundation for Basic Research (04-03-32277).

References and Notes

(1) Dawson, J. H. *Science* **1988**, *240*, 433−439.

(2) Schlichting, I.; Berendzen, J.; Chu, K.; Stock, A. M.; Maves, Sh. A.; Benson, D. K.; Sweet, R. M.; Ringe, D.; Petsko, G. A.; Sligar, S. G. *Science* **2000**, *287*, 1615−1622.

(3) Salikhov, K. M.; Molin, Yu. N.; Sagdeev, R. Z.; Buchachenko, A. L. *Spin Polarization and Magnetic Effects in Radical Reactions*; Elsevier: Amsterdam, 1984.

(4) Gębicki, J.; Marcinek, A.; Zielonka, J. *Acc. Chem. Res.* **2004**, *37*, 379−386.

(5) Lee, I.-S. H.; Jeoung, E. H.; Kreevoy, M. M. *J. Am. Chem. Soc.* **1997**, *119*, 2722−2728.

(6) Carlson, B. W.; Miller, L. L.; Neta, P.; Grodkowski, J. *J. Am. Chem. Soc.* **1984**, *106*, 7233−7239.

(7) Almarsson, Ö.; Sinha, A.; Gopinath, E.; Bruice, T. C. *J. Am. Chem. Soc.* **1993**, *115*, 7093−7102.

(8) Møller, A. C.; Lunding, A.; Olsen, L. F. *Phys. Chem. Chem. Phys.* **2000**, *2*, 3443−3446.

(9) Afanasyeva, M. S.; Taraban, M. B.; Purtov, P. A.; Leshina, T. V.; Grissom, C. B. *J. Am. Chem. Soc*. **2006**, *128*, 8651−8658.

(10) Taraban, M. B.; Kruppa, A. I.; Polyakov, N. E.; Leshina, T. V.; Lūsis, V.; Muceniece, D.; Duburs, G. *J. Photochem. Photobiol. A: Chem*. **1993**, *73*, 151−157.

(11) Kruppa, A. I.; Taraban, M. B.; Polyakov, N. E.; Leshina, T. V.; Lūsis, V.; Muceniece, D.; Duburs, G. *J. Photochem. Photobiol. A: Chem*. **1993**, *73*, 159−163.

(12) Polyakov, N. E.; Taraban, M. B.; Kruppa, A. I.; Avdievich, N. I.; Mokrushin, V. V.; Schastnev, P. V.; Leshina, T. V.; Lūsis, V.; Muceniece, D.; Duburs, G. *J. Photochem. Photobiol. A: Chem*. **1993**, *74*, 75−79.

(13) Polyakov, N. E.; Kruppa, A. I.; Leshina, T. V.; Lūsis, V.; Muceniece, D.; Duburs, G. *J. Photochem. Photobiol. A: Chem*. **1997**, *111*, 61−64.

(14) Scheeline, A.; Olson, D. L.; Williksen, E. P.; Horras, G. A.; Klein, M. L.; Larter, R. *Chem. Rev*. **1997**, *97*, 739−756.

(15) Ataullakhanov, F. I.; Zhabotinsky, A. M. *Biofizika* **1975**, *20*, 596−601.

(16) Harkins, T. T.; Grissom, C. B. *J. Am. Chem. Soc.* **1995**, *117*, 566−568.

(17) Yokota, K.; Yamazaki, I. *Biochemistry*, **1977**, *16*, 1913−1920.

(18) Hore, P. J.; Volbeda, A.; Dijkstra, K.; Kaptein, R. *J. Am. Chem. Soc*. **1982**, *104*, 6262−6267.